

Quantum phase transition in Bose-Holstein model in two dimensions

Sanjoy Datta* and Sudhakar Yarlagadda†

Saha Institute of Nuclear Physics, 1/AF-Bidhannagar, Kolkata-64, India

(Dated: November 7, 2018)

We derive an effective d-dimensional Hamiltonian for a system of hard-core-bosons coupled to optical phonons in a lattice. Away from half-filling, we show that the presence of next-nearest-neighbor hopping in the effective Hamiltonian leads to a superfluid-to-supersolid transition at intermediate boson-phonon (b-p) couplings, while at strong-couplings the system phase separates. However, at half-filling and at a critical b-p coupling (as in the xxz-model), the system undergoes a superfluid-to-charge-density-wave transition without any signature of supersolidity. Our analyses is based on extensive calculations of the structure factor, the superfluid fraction, the Bose-Einstein condensate fraction, and the system energy at various fillings. We present a phase diagram for this system and compare it to that of the xxz-model. We also demonstrate explicitly that the next-nearest-neighbor hopping (in the absence of nearest-neighbor hopping) in the effective Hamiltonian leads only to a single transition – a first-order superfluid-to-supersolid transition.

PACS numbers:

I. INTRODUCTION

The successful mimicking of an actual lattice using optical standing waves marks one of the most significant scientific advances of this decade¹. The biggest advantage of this kind of an optical lattice is that the ratio of the kinetic energy and the interaction energy of the particles can be controlled at will. This has led to a flurry of activities among atomic and condensed matter physicists across the world. The excitement among the condensed matter physicists stems from the fact that it not only gives a testing ground for some of the most intriguing phenomena of nature predicted earlier, but it also paves the way for the discovery of new physical phenomena. For example, soon after the creation of a two dimensional (2D) optical lattice, it has been used to experimentally verify² the predicted transition³ from a superfluid state to a Mott insulating state of a bosonic system. Another possibility is the verification of the theoretically predicted supersolidity due to vacancies^{4,5,6}. A signature of supersolidity is the simultaneous presence of both diagonal long range order (DLRO) and off diagonal long range order (ODLRO)^{7,8}. There have not been many studies of this interesting phase of matter until it was recently observed in helium-4^{9,10}. This discovery led theorists to study bosonic models in different kinds of lattice structures^{11,12,13}. and with various types of interactions among these particles¹⁴.

There has been very little attention given to a system of bosons interacting with phonons. Recently Pupillo *et al.*¹⁵ have studied such a possibility where the bosons could be coupled to the acoustic phonons generated by polar molecules trapped to form a lattice. In this paper, we have considered a Bose-Holstein model compris-

ing of hard-core-bosons (hcb) coupled to optical phonons generated by the vibrations of the underlying lattice. An example of such hcb is a collection of tightly-bound Cooper pairs originating from electronic polarization processes^{16,17}. Additionally, strong-coupling between electrons and intermolecular-phonons also produces hcb; when such hcb couple to intra-molecular phonons, the system can be studied by a Bose-Holstein model¹⁸. Starting with a minimalistic model, involving momentum independent b-p coupling, we have derived an effective d-dimensional Hamiltonian for hcb by using a transparent non-perturbative technique. The region of validity of our effective Hamiltonian is governed by the small parameter ratio of the adiabaticity t/ω_0 and the b-p coupling g . The most interesting feature of this effective Hamiltonian is that, besides a nearest-neighbor (NN) hopping, it consists of next-nearest-neighbor (NNN) hopping and NN repulsion. Our approach gives a microscopic justification for the origin of these important additional terms. We study our derived effective Hamiltonian in 2D by using exact diagonalization technique. For exact diagonalization, we have used a modified Lanczos algorithm¹⁹ on lattice clusters with 4×4 , $\sqrt{18} \times \sqrt{18}$, and $\sqrt{20} \times \sqrt{20}$ sites. We have shown that, except for the extreme anti-adiabatic limit, the hcb coupled with optical phonons can show supersolidity above a critical value of the b-p coupling strength.

The paper has been arranged as follows. In Sec. II, we have derived the effective Hamiltonian for a system of hcb coupled to optical phonons. We discuss briefly the basic difference of this effective Hamiltonian with that for fermions²⁰. Next, we apply mean field analysis to this Hamiltonian in Sec. III and obtain a mean field phase diagram. In Sec. IV, we discuss in detail the DLRO by studying the structure factor. Here, we also present key numerical results. In Sec. V, we discuss two important quantities – the Bose condensate fraction and the superfluid fraction. Sec. VI deals with calculating the free energy of the system for different situations and param-

*Electronic address: sanjoy.datta@saha.ac.in

†Electronic address: y.sudhakar@saha.ac.in

ter values. The curvature of the free-energy-versus-filling curves is used in deciding whether the system phase separates or not. Finally, in Sec. VII, we present the results.

II. EFFECTIVE HAMILTONIAN

We start with a system of spinless hcb coupled with optical phonons on a square lattice. This system is described by a Bose-Holstein Hamiltonian²¹

$$H_{\text{hol}} = -t \sum_{j,\delta} b_{j+\delta}^\dagger b_j + \omega_0 \sum_j a_j^\dagger a_j + g\omega_0 \sum_j n_j (a_j + a_j^\dagger), \quad (1)$$

where δ corresponds to nearest-neighbors, $n_j \equiv b_j^\dagger b_j$ with b_j being the destruction operator for hcb (and not of electrons as in the Holstein model), while (as in the Holstein case) a_j is the destruction operator for phonons, and ω_0 is the single vibrational frequency for simple harmonic oscillators. Then we perform the Lang-Firsov (LF) transformation²² on this Hamiltonian which produces displaced simple harmonic oscillators and dresses the hopping particles with phonons. It is important to note that although we are dealing with particles different from fermions, we can still perform the same LF transformation. This is because, under the LF transformation given by $e^S H_{\text{hol}} e^{-S}$ with $S = -g \sum_i n_i (a_i - a_i^\dagger)$, b_j and a_j transform (like fermions and phonons in the Holstein model) as follows:

$$\begin{aligned} \tilde{b}_j &\equiv e^S b_j e^{-S} = b_j e^{-g(a_j - a_j^\dagger)}, \\ \tilde{a}_j &\equiv e^S a_j e^{-S} = a_j - g n_j. \end{aligned} \quad (2)$$

This is due to the unique (anti-) commutation properties of hcb given by

$$\begin{aligned} [b_i, b_j] &= [b_i, b_j^\dagger] = 0, \text{ for } i \neq j, \\ \{b_i, b_i^\dagger\} &= 1. \end{aligned} \quad (3)$$

Next, we take the unperturbed Hamiltonian to be given by²⁰

$$H_0 = \omega_0 \sum_j a_j^\dagger a_j - g^2 \omega_0 \sum_j b_j^\dagger b_j - J_1 \sum_j (b_j b_{j+\delta} + \text{H.c.}), \quad (4)$$

and the perturbation to be

$$H' = \sum_j H_j = -J_1 \sum_j (b_j^\dagger b_{j+\delta} \{S_+^j S_-^j - 1\} + \text{H.c.}), \quad (5)$$

where $S_\pm^j = \exp[\pm g(a_j - a_{j+\delta})]$, $J_1 = t \exp(-g^2)$, and $g^2 \omega_0$ is the polaronic binding energy. Here, $H_0 + H'$ constitutes the LF transformed Bose-Holstein Hamiltonian. We then follow the same steps as in Ref. [20] to get the following effective Hamiltonian in d-dimensions for our

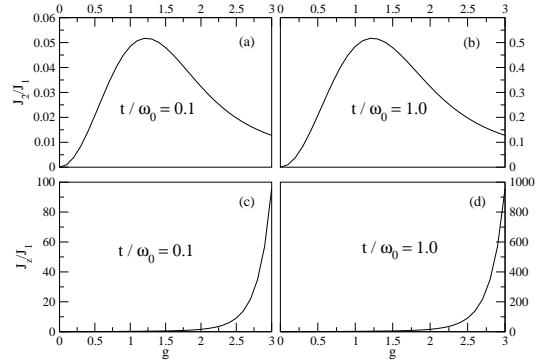


FIG. 1: Comparison of J_2/J_1 and J_z/J_1 at two different values of t/ω_0 and various values of g .

Bose-Holstein model

$$\begin{aligned} H_{\text{eff}} &= -g^2 \omega_0 \sum_j n_j - J_1 \sum_{j,\delta} b_j^\dagger b_{j+\delta} \\ &\quad - J_2 \sum_{j,\delta,\delta' \neq \delta} b_{j+\delta'}^\dagger b_{j+\delta} - 0.5 J_z \sum_{j,\delta} n_j (1 - n_{j+\delta}), \end{aligned} \quad (6)$$

where $J_z \equiv (J_1^2/\omega_0)[4f_1(g) + 2f_2(g)]$ and $J_2 \equiv (J_1^2/\omega_0)f_1(g)$ with $f_1(g) \equiv \sum_{n=1}^{\infty} g^{2n}/(n!n)$ and $f_2(g) \equiv \sum_{n=1}^{\infty} \sum_{m=1}^{\infty} g^{2(n+m)}/[n!m!(n+m)]$. In Fig. 1, we plot the ratios J_2/J_1 and J_z/J_1 for various values of g and adiabaticity parameter t/ω_0 . We note that both $(J_2/J_1) \times (\omega_0/t)$ and $(J_z/J_1) \times (\omega_0/t)$ are functions of g only.

The effective Hamiltonian in Eq. (6) is different from that for spinless fermions in Ref. [20]. This is because the effective Hamiltonian for fermions contains an *extra correlated hopping term* $J_2 \sum_{j,\delta,\delta' \neq \delta} 2n_j c_{j+\delta'}^\dagger c_{j+\delta}$ (with c_j being the destruction operator for fermions) because the commutation relations for fermions are different from those of hcb given in Eq. (3). To see the difference clearly, let us consider the simplest case of one-dimension (1D). After carrying out the second-order perturbation theory for fermions (bosons), we get in 1D the term $c_{j-1}^\dagger c_j c_{j+1}^\dagger (b_{j-1}^\dagger b_j b_j^\dagger b_{j+1})$ depicted by the process (a) in Fig. 2 and the term $c_j^\dagger c_{j+1} c_{j-1}^\dagger c_j (b_j^\dagger b_{j+1} b_{j-1}^\dagger b_j)$ depicted by the process (b) in Fig. 2. For fermions, when these two terms are added, one gets $c_{j-1}^\dagger (1 - 2n_j) c_{j+1}$ whereas for bosons one gets only $b_{j-1}^\dagger b_{j+1}$. These arguments can easily be extended to d-dimensions. In a previous work²³, while performing a similar second-order perturbation theory, the authors missed the process depicted in Fig. 2(b). Here we would like to point out that, as mentioned in Ref. 24, the small parameter for our perturbation theory is $t/(g\omega_0)$.

III. MEAN FIELD ANALYSIS

In this section, we shall study the phase transitions dictated by the effective Hamiltonian of Eq. (6) by em-

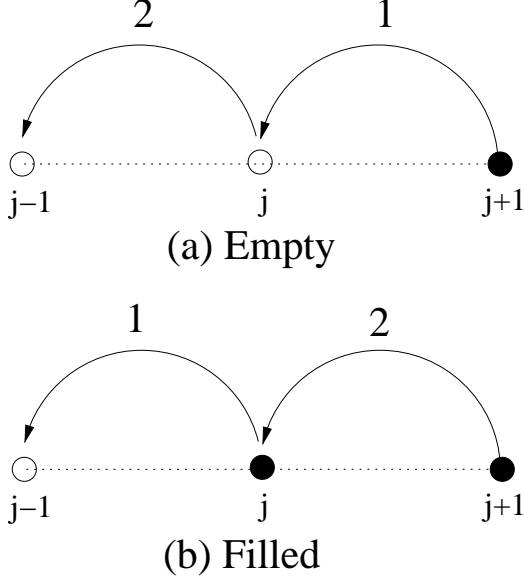


FIG. 2: Depicted processes describe the following terms: (a) $c_{j-1}^\dagger c_j c_{j+1}^\dagger$ when site j is empty; and (b) $c_j^\dagger c_{j+1} c_{j-1}^\dagger c_j$ for a filled site j

employing the mean field analysis (MFA) of Robaszkiewicz *et al.*²⁵. We first note that the hcb may be represented by spin one-half operators. More precisely, with the transformations $S^+ = S^x + iS^y = b^\dagger$, $S^- = S^x - iS^y = b$, and $S^z + 0.5 = b^\dagger b$, the commutation relations of Eq. (3) are preserved. We can then write the Hamiltonian of Eq. (6) in the following form:

$$\begin{aligned}
H_0 = & -J_1 \sum_{j,\delta} (S_j^x S_{j+\delta}^x + S_j^y S_{j+\delta}^y) \\
& -J_2 \sum_{j,\delta,\delta',\delta \neq \delta'} (S_{j+\delta'}^x S_{j+\delta}^x + S_{j+\delta'}^y S_{j+\delta}^y) \\
& + 0.5 J_z \sum_{j,\delta} S_j^z S_{j+\delta}^z - B \sum_j (2S_j^z + 1), \quad (7)
\end{aligned}$$

with the constraint

$$\frac{1}{N} \sum_i \langle S_i^z \rangle = \frac{1}{2} (2n - 1), \quad (8)$$

where N is the number of sites in the lattice. Here, $B = J_z/2 + g^2 \omega_0/2$ is the effective magnetic field and $n = \frac{1}{N} \sum_i \langle b_i^\dagger b_i \rangle$ is the filling fraction ($0 \leq n \leq 1$). In the MFA, for a trial Hamiltonian H_0 the following identity holds:

$$F \leq F_0 = -\frac{1}{\beta} \ln \text{Tr} [\exp(-\beta H_0)] + \langle H - H_0 \rangle_0, \quad (9)$$

where $\beta = 1/k_B T$ and $\langle \dots \rangle_0$ is the thermal average with respect to the trial Hamiltonian H_0 . The trial Hamilto-

nian H_0 is chosen as

$$H_0 = - \sum_i \vec{\Lambda}_i \cdot \vec{S}_i - B \sum_i 1, \quad (10)$$

where the molecular fields $\vec{\Lambda}_i$ are obtained variationally by minimizing F_0 . After some standard calculation, we obtain

$$\begin{aligned}
\Lambda_i^x = \Lambda_i^y &= 2 \sum_\delta J_1 \langle S_{i+\delta}^x \rangle_0 + 2 \sum_{\delta,\delta',\delta \neq \delta'} J_2 \langle S_{i+\delta-\delta'}^x \rangle_0 \\
\Lambda_i^z &= 2B - \sum_\delta J_z \langle S_{i+\delta}^z \rangle_0. \quad (11)
\end{aligned}$$

The eigenenergies of Eq. (10) are

$$\lambda = -B \pm \Delta_\zeta, \quad (12)$$

where

$$\Delta_\zeta = \sqrt{\left(\frac{\Lambda_\zeta^z}{2}\right)^2 + \left(\frac{\Lambda_\zeta^x}{2}\right)^2}. \quad (13)$$

Here $\zeta = a, b$ represents the two sub-lattices. The eigenfunctions are given by

$$\begin{aligned}
\psi_\zeta^+ &= \cos\left(\frac{\theta_\zeta}{2}\right) \left| \frac{1}{2} \right\rangle + \sin\left(\frac{\theta_\zeta}{2}\right) \left| -\frac{1}{2} \right\rangle \\
\psi_\zeta^- &= -\sin\left(\frac{\theta_\zeta}{2}\right) \left| \frac{1}{2} \right\rangle + \cos\left(\frac{\theta_\zeta}{2}\right) \left| -\frac{1}{2} \right\rangle, \quad (14)
\end{aligned}$$

where $\sin\theta_\zeta = \frac{\Lambda_\zeta^x}{2\Delta_\zeta}$ and $\cos\theta_\zeta = \frac{\Lambda_\zeta^z}{2\Delta_\zeta}$. At $T = 0K$, ground state expectation value of S_x and S_z are given by

$$\langle S_\zeta^x \rangle_0 = \frac{\sin\theta_\zeta}{2}, \quad (15)$$

and

$$\langle S_\zeta^z \rangle_0 = \frac{\cos\theta_\zeta}{2}. \quad (16)$$

Now, to obtain the ground-state phase diagram we calculate the ground-state energy to be

$$\begin{aligned}
E_g &= \frac{\langle H \rangle_0}{J_1' N} \\
&= -\frac{1}{4} \sin\theta_a \sin\theta_b - \frac{J_2'}{8J_1'} \sin^2\theta_a - \frac{J_2'}{8J_1'} \sin^2\theta_b + \\
&\quad \frac{J_z'}{8J_1'} \cos\theta_a \cos\theta_b - \frac{B}{2J_1'} [\cos\theta_a + \cos\theta_b + 2], \quad (17)
\end{aligned}$$

where $J_1' \equiv Z_{nn} J_1$, $J_2' \equiv Z_{nnn} J_2$, and $J_z' \equiv Z_{nn} J_z$, with Z_{nn} and Z_{nnn} being the number of nearest-neighbor (NN) and next-nearest-neighbor (NNN) hopping processes respectively. For the Hamiltonian of Eq.(6), $Z_{nn} = 4$ while $Z_{nnn} = 12$ because of the diagonal hoppings given by the

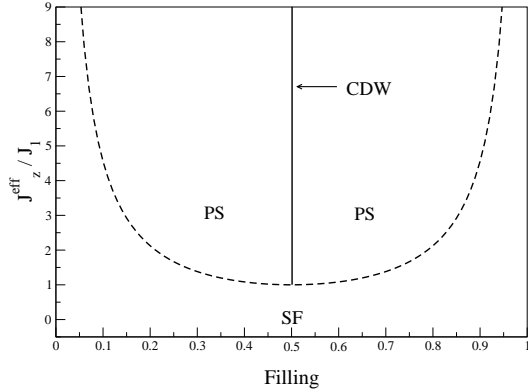


FIG. 3: Mean field phase diagram with $J_z^{eff} = J_z/2 - 3J_2$.

third term on the right-hand-side of Eq.(6). Minimization of E_g , with respect to θ_a and θ_b , gives the following two conditions:

$$\begin{aligned} 2B\sin\theta_a &= J'_1\cos\theta_a\sin\theta_b + J'_2\sin\theta_a\cos\theta_a + 0.5J'_z\sin\theta_a\cos\theta_b \\ 2B\sin\theta_b &= J'_1\cos\theta_b\sin\theta_a + J'_2\sin\theta_b\cos\theta_b + 0.5J'_z\sin\theta_b\cos\theta_a. \end{aligned} \quad (18)$$

Now we note that, for a charge density wave (CDW) state we have $(\theta_a, \theta_b) = (0, \pi)$ or $(\theta_a, \theta_b) = (\pi, 0)$; for a superfluid (SF) state $\theta_a = \theta_b$; and for a phase separated (PS) regime $\theta_a \neq \theta_b$ and $\theta_{a,b} \neq 0$ or π . Then, from Eq.(18), we obtain the following expression for the phase boundary:

$$\frac{J'_z}{2J'_1} - \frac{J'_2}{J'_1} = \frac{J_z}{2J_1} - \frac{3J_2}{J_1} = \frac{1 + (2n-1)^2}{1 - (2n-1)^2}. \quad (19)$$

From Eq. (19), we see that we obtain the mean-field phase boundary of Ref. [25] when $J'_2 = 0$. We further note that NNN hopping does not change the qualitative feature of the phase diagram (see Fig. 3); it only increases the critical value of J_z/J_1 at which the transition from SF state to PS or CDW state occurs.

IV. DIAGONAL LONG RANGE ORDER AND STRUCTURE FACTOR

Diagonal long range order (DLRO) is the typical property of a crystalline solid and information about the periodicity in the solid is contained in the structure factor. For crystalline solids, the structure factor shows delta function peak at the reciprocal lattice points. In terms of the particle density operators the structure factor is given by

$$S(\mathbf{q}) = \sum_{\mathbf{i}, \mathbf{j}} \mathbf{e}^{i\mathbf{q} \cdot (\mathbf{R}_i - \mathbf{R}_j)} (\langle \mathbf{n}_i \mathbf{n}_j \rangle - \langle \mathbf{n}_i \rangle \langle \mathbf{n}_j \rangle). \quad (20)$$

In this paper, we have calculated the structure factor using exact diagonalization technique for lattice clusters of size 4×4 , $\sqrt{18} \times \sqrt{18}$, and $\sqrt{20} \times \sqrt{20}$.

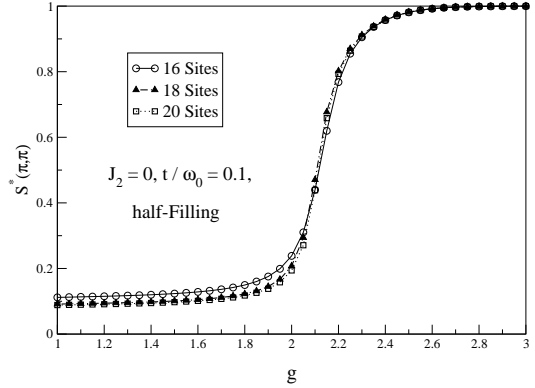


FIG. 4: Normalized structure factor $S^*(\pi, \pi) = S(\pi, \pi)/S^{max}(\pi, \pi)$ for three different lattice clusters at half-filling. Here, adiabaticity parameter $t/\omega_0 = 0.1$ and NNN hopping $J_2 = 0$.

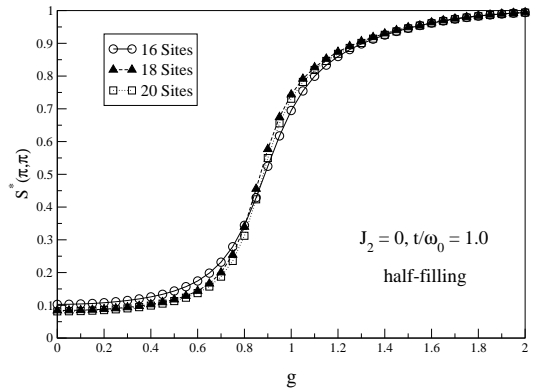


FIG. 5: Depiction of $S^*(\pi, \pi)$ for three different lattice clusters at half-filling with $t/\omega_0 = 1.0$ and $J_2 = 0$.

A. $J_2 = 0$

We will now present the structure factor results when $J_2 = 0$, i.e., for the xxz-model. In Fig. 4, we have plotted the normalized structure factor $S^*(\pi, \pi) = S(\pi, \pi)/S^{max}(\pi, \pi)$ where $S^{max}(\pi, \pi)$ corresponds to all particles in only one sub-lattice. The calculations were done at half-filling and for different lattice clusters with the adiabaticity parameter $t/\omega_0 = 0.1$. From Fig. 4, we see that, at half-filling, the system makes a transition to a CDW state at a critical b-p coupling strength $g_c \approx 2.15$.

On the other hand, at a larger $t/\omega_0 = 1.0$, the transition for a half-filled system occurs at a significantly lower value of $g_c \approx 0.9$ (see Fig. 5). This is because, for $J_2 = 0$, the transition is governed only by the ratio J_z/J_1 . Since $(J_z/J_1) \times (\omega_0/t)$ is a monotonically increasing function of g , for a larger value of t/ω_0 , it takes a lower value of g to attain the same value of J_z/J_1 . Another important point to note from Figs. 4 and 5 is that $S^*(\pi, \pi)$ is almost identical for different lattice clusters. The jump in the structure factor becomes sharper as we increase the system size. However this does not change the point of

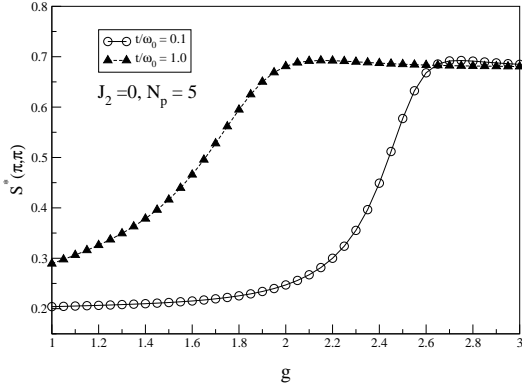


FIG. 6: Comparison of $S^*(\pi, \pi)$ values for $t/\omega_0 = 0.1$ & 1.0 . Plots are for 5 particles in a 4×4 lattice and $J_2 = 0$.

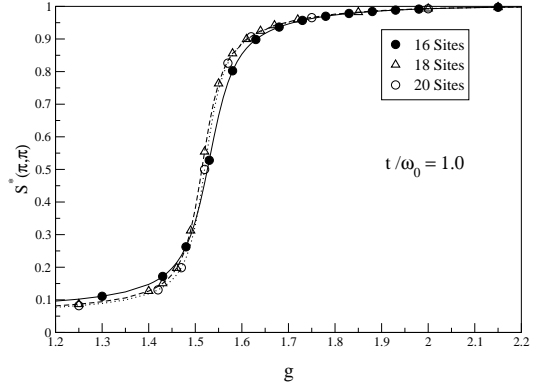


FIG. 8: Plots of $S^*(\pi, \pi)$ for three different lattice clusters at half-filling, $t/\omega_0 = 1.0$, and $J_2 \neq 0$.

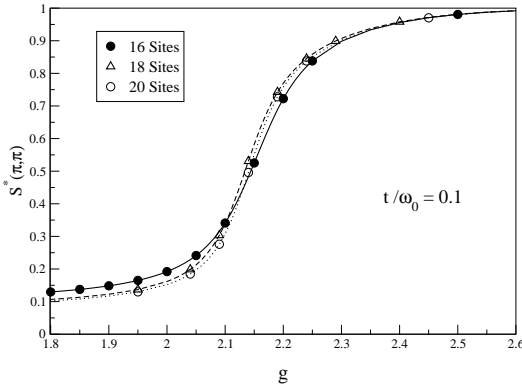


FIG. 7: $S^*(\pi, \pi)$ for three different lattice clusters at half-filling, extreme adiabaticity ($t/\omega_0 = 0.1$), and non-zero NNN hopping J_2 .

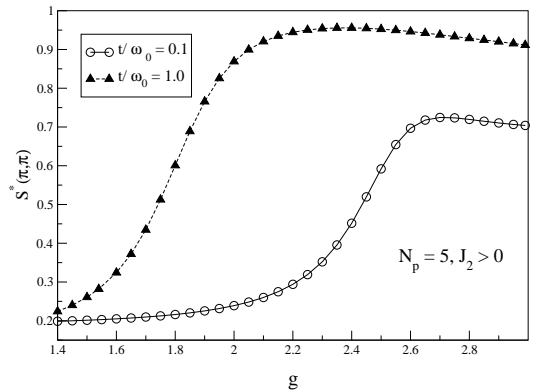


FIG. 9: Comparison of $S^*(\pi, \pi)$ plots at two extreme values of t/ω_0 . Figures are for 5 particles in a 4×4 lattice cluster and $J_2 \neq 0$.

transition significantly. This means that the 4×4 lattice cluster is enough to have a reasonable estimate of the transition point.

Next, we proceed to analyze the system away from half-filling. Without actually presenting the details of the calculations, we first note that, for $N_p \leq 4$ in a 4×4 lattice, there is no evidence of a phase transition. Here, we present the results for total number of particles $N_p = 5$ in a 4×4 cluster. From Fig. 6, we see that the qualitative features of the transition are similar to those of the half-filled case. However, in detail, the two cases differ in the following sense. Firstly, the critical values of the b-p coupling are larger for $N_p = 5$ with $g_c \approx 2.45$ for $t/\omega_0 = 0.1$, while $g_c \approx 1.70$ for $t/\omega_0 = 1.0$. Secondly, the 5-particle system never attains a fully CDW-state as seen from $S^*(\pi, \pi)$ being noticeably less than unity. Lastly, in Fig. 6, we see that $S^*(\pi, \pi)$ decreases slowly after attaining a peak value which is perhaps due to some special correlations which need to be examined.

B. $J_2 \neq 0$

In this sub-section, we shall consider the effect of the additional NNN hopping J_2 . At half filling, for a small value of the adiabaticity parameter $t/\omega_0 = 0.1$, we find that the system undergoes a phase transition from a SF-state to a CDW-state at a critical boson-phonon coupling strength $g_c \approx 2.16$ (see Fig. 7) which is very close to the case when $J_2 = 0$ (see Fig. 4). This is because, when t/ω_0 is small, the ratio $J_2/J_1 \ll 1$ for all values of g (see Fig. 1).

When we increase the value of t/ω_0 , as is evident from Fig. 8, the value of the critical coupling g_c decreases. The physical reason for this has already been discussed in section IV A. At half-filling, for $t/\omega_0 = 1.0$, we find $g_c \approx 1.53$. Furthermore, for a given value of t/ω_0 , the system makes a transition to the CDW state at a lower value of g when NNN hopping $J_2 = 0$. This is in accordance with the mean field analysis, which shows that the presence of J_2 delays the transition [see Eq. (19)]. This is because, for relevant values of g , when $t/\omega_0 = 1$, the J_2/J_1 term is small but not negligible. Presence of J_2 introduces disorder in the system. Hence, it takes a higher

J_z/J_1 ratio (i.e., a higher value of g) to make the system ordered. Similar to the $J_2 = 0$ case in a 4×4 lattice, we also find that for fillings up to 0.25 there is no transition to a CDW state while a CDW transition does occur for 5 hcb. For $N_p = 5$, as seen from Fig. 9, $g_c \approx 2.45$ for $t/\omega_0 = 0.1$ while $g_c \approx 1.85$ for $t/\omega_0 = 1.0$.

V. OFF-DIAGONAL LONG RANGE ORDER

The concept of off-diagonal long range order (ODLRO) was introduced by Penrose and Onsager⁷ to understand the nature of the order in superfluids. Bose-Einstein condensate is one example which shows ODLRO. Following Refs. [26] and [27], we define the general one-particle density matrix as

$$\tilde{\rho}(i, j) = \langle b_i^\dagger b_j \rangle = \frac{1}{N} \sum_{\mathbf{k}, \mathbf{q}} e^{i(\mathbf{k} \cdot \mathbf{R}_i - \mathbf{q} \cdot \mathbf{R}_j)} \langle b_{\mathbf{k}}^\dagger b_{\mathbf{q}} \rangle. \quad (21)$$

Here $\langle \rangle$ denotes ensemble average and $b_{\mathbf{k}}^\dagger$ is the creation operator for hcb in momentum space. It is easy to see that $\tilde{\rho}$ becomes the diagonal one-particle density matrix when $i = j$.

A. Condensate fraction

It follows from Eq. (21) that, for a translationally invariant system,

$$\sum_j \tilde{\rho}(i, j) = \langle n_0 \rangle, \quad (22)$$

where n_0 is the occupation number for the $\mathbf{k} = 0$ momentum state. Eq. (21) gives the Bose-Einstein condensate fraction as

$$n_b = \sum_{i,j} \frac{\tilde{\rho}(i, j)}{NN_p}. \quad (23)$$

In general, to find n_b , one constructs the generalized one-particle density matrix $\tilde{\rho}$ and then diagonalizes it to find out the largest eigenvalue. This procedure alone does not tell us which momentum state corresponds to the largest eigenvalue. To find out whether the $\mathbf{k} = 0$ momentum state is macroscopically occupied or not, we proceed as follows. First let us see if $\langle n_0 \rangle$ is one of the eigenvalues. For this consider the following single-particle generalized density matrix,

$$\tilde{\rho} = \begin{pmatrix} \tilde{\rho}(1, 1) & \tilde{\rho}(1, 2) & \cdots & \tilde{\rho}(1, N) \\ \tilde{\rho}(2, 1) & \tilde{\rho}(2, 2) & \cdots & \tilde{\rho}(2, N) \\ \vdots & \vdots & \ddots & \vdots \\ \tilde{\rho}(N, 1) & \tilde{\rho}(N, 2) & \cdots & \tilde{\rho}(N, N) \end{pmatrix},$$

which can be re-written as

$$\tilde{\rho} = \begin{pmatrix} \sum_i \tilde{\rho}(i, 1) & \sum_i \tilde{\rho}(i, 2) & \cdots & \sum_i \tilde{\rho}(i, N) \\ \tilde{\rho}(2, 1) & \tilde{\rho}(2, 2) & \cdots & \tilde{\rho}(2, N) \\ \vdots & \vdots & \ddots & \vdots \\ \tilde{\rho}(N, 1) & \tilde{\rho}(N, 2) & \cdots & \tilde{\rho}(N, N) \end{pmatrix}. \quad (24)$$

From Eq. (24), it is easy to see that, for a translationally invariant system, $\langle n_0 \rangle$ is indeed an eigenvalue of the one-particle generalized density matrix. We found in our calculations that, for all the relevant regions of the various parameter spaces, the value of $\langle n_0 \rangle$ obtained according to Eq. (22) and the highest eigenvalue of the density matrix coincide quite accurately.

B. Superfluid fraction

To characterize a superfluid, another important quantity of interest is the superfluid fraction n_s . The order parameter for a superfluid is a complex number and it is taken to be $\langle b \rangle = \sqrt{\langle n_0 \rangle} / N e^{i\theta}$ where the lattice constant has been taken to be unity. Spatial variation in the phase θ will increase the free energy (or simply the energy at $T = 0$) of the system. We consider an imposed phase variation that is a linear function of the phase angle, i.e., we take $\theta(x) = \theta_0 \frac{x}{L}$ where L is the linear dimension of the system along the x -direction. For simplicity we have chosen the variation in θ to be only along the x -direction. With these considerations we can write the change in energy to be

$$E[\theta_0] - E[\theta = 0] = \frac{1}{2} m N_p n_s \left| \frac{\hbar}{m} \vec{\nabla} \theta(x) \right|^2, \quad (25)$$

where $E[\theta_0]$ corresponds to an imposed phase variation when $\theta_0 \neq 0$. Here, it is important to note that θ_0 should be small, because a larger θ_0 can induce other excitations which can destroy the collective motion of the superfluid component (see Ref. [28] and the references therein for details). We then get the superfluid fraction to be

$$n_s = \left(\frac{N}{N_p t_{eff}} \right) \frac{E[\theta_0] - E[\theta = 0]}{\theta_0^2}, \quad (26)$$

where $t_{eff} = \hbar^2/2m$. For our Hamiltonian in Eq. (6), we find $t_{eff} = J_1 + 8J_2$. Now, to introduce the phase variation, we impose twisted boundary conditions on the many-particle wave function. A twist in the boundary conditions is gauge-equivalent to modifying the hopping terms in the Hamiltonian of Eq. (6). With this modification, the effective Hamiltonian becomes

$$\begin{aligned} H_\theta = & -g^2 \omega_0 \sum_j n_j - J_1 \sum_{j, \delta} e^{i\theta \hat{x} \cdot (\mathbf{R}_j - \mathbf{R}_{j+\delta})} b_j^\dagger b_{j+\delta} \\ & - J_2 \sum_{j, \delta, \delta' \neq \delta} e^{i\theta \hat{x} \cdot (\mathbf{R}_{j+\delta'} - \mathbf{R}_{j+\delta})} b_{j+\delta'}^\dagger b_{j+\delta} \\ & - 0.5 J_z \sum_{j, \delta} n_j (1 - n_{j+\delta}), \end{aligned} \quad (27)$$

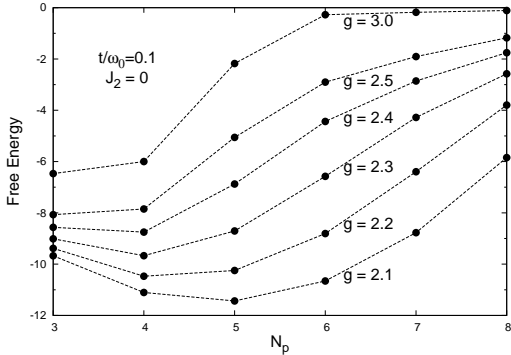


FIG. 10: Free energy plots at different fillings for $J_2 = 0$, $t/\omega_0 = 0.1$, and various b-p couplings g .

where \hat{x} is a unit vector in the x -direction.

VI. ENERGY CONSIDERATION

In this section, we shall examine the possibility of phase separation for the system of hcb coupled with optical phonons. To this end, we have calculated the free energy for different number of particles in a 4×4 lattice. In Sec. IV, for both $J_2 = 0$ and $J_2 > 0$, we observed that the system is always a pure superfluid for $N_p \leq 4$ in a 4×4 lattice and that it is either a pure CDW or a pure superfluid at half-filling. After plotting the free energy at different fillings, if it is found that the curve is convex at a given filling, then the system at that filling is said to be stable; whereas, if the curve is concave at that filling, then the system would be unstable against phase separation. This procedure of calculating free energy at various fillings to figure out the stability of a system is equivalent to the well-known *Maxwell construction*.

A. $J_2 = 0$

In Sec. IV A we saw that, at half-filling, $J_2 = 0$, and $t/\omega_0 = 0.1$, the system makes a transition to a CDW state at $g \approx 2.15$. From Fig. 10, we see that for $g \leq 2.2$, the system in between quarter-filling and half-filling is stable due to the convexity of the energy curve here. As g is increased, the system close to half-filling becomes unstable first and then the lower-fillings becoming unstable progressively. For $J_2 = 0$, we see from Figs. 10 and 11 that the qualitative nature of the free energy curves, with respect to phase separation, does not depend on the adiabaticity parameter. As expected from the explanation in Sec. IV, these figures show that the critical value g_c (where the phase separation starts) decreases as t/ω_0 increases. We notice in Fig. 10 (Fig. 11) that, for $N_p = 7, 6, \& 5$, the energy curves become concave before $g = 2.3, 2.4, \& 2.5$ ($g = 1.2, 1.4, \& 1.7$) respectively. Furthermore, for $N_p = 5$, the phase separation seems to

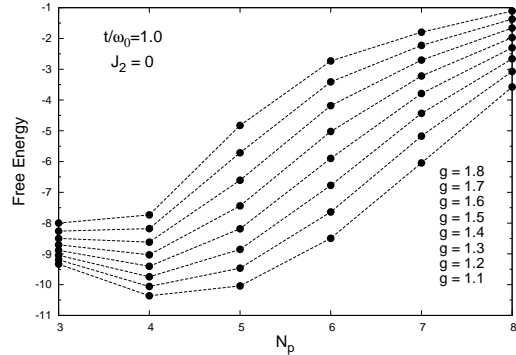


FIG. 11: Free energy versus particle number N_p for parameters $J_2 = 0$, $t/\omega_0 = 1.0$, and g at different values.

occur at approximately the same value of g at which the CDW transition occurs (see Fig. 6).

B. $J_2 \neq 0$

For the extreme anti-adiabatic regime, the situation, when NNN hopping $J_2 \neq 0$, is not too different from the $J_2 = 0$ case. This can be seen by comparing Figs. 12 and 10 drawn for $t/\omega_0 = 0.1$. This is expected because, for the extreme anti-adiabatic regime, the ratio $J_2/J_1 \ll 1$. However, when $t/\omega_0 = 1.0$ (J_2/J_1 ratio is not negligible at values of g considered in Fig. 13), the situation is quite different from the $J_2 = 0$ case away from half-filling. In Fig. 9, we saw that the structure factor revealed a CDW transition at $g_c \approx 1.85$ for $N_p = 5$. However, for $J_2 \neq 0$, the phase separation occurs at a higher value of $g \approx 2.1$ as can be seen from Fig. 13. The interesting implications of the CDW transition occurring before the PS transition will be discussed in the next section.

One additional important feature for the $J_2 \neq 0$ case, compared to the $J_2 = 0$ case, is that the phase separation first occurs at the low-filling side. For 6 particles, the phase separation sets in at $g \approx 3.0$; while for 7 particles the corresponding g -value is expected to be even higher. We could not obtain the exact g -value for PS instability for $N_p = 7$ as our code had convergence problems when we tried to go beyond $g = 3.0$.

VII. RESULTS AND DISCUSSIONS

Here, we will analyze together, in one plot, the quantities $S^*(\pi, \pi)$, n_b and n_s that were presented in earlier sections. For a half-filled system at $J_2 = 0$ and $t/\omega_0 = 0.1$ ($t/\omega_0 = 1.0$), we can see from Fig. 14 (Fig. 15) that the system undergoes a sharp transition to an insulating CDW state at $g_c \approx 2.15$ ($g_c \approx 0.9$). At $g = g_c$, while there is a sharp rise in the structure factor $S(\pi, \pi)$, there is also a concomitant sharp drop in both the condensation fraction n_b and the superfluid fraction n_s . Furthermore,

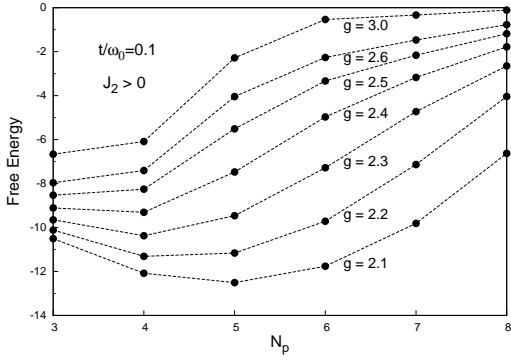


FIG. 12: Free energy at different fillings for $t/\omega_0 = 0.1$ and different values of g . Here NNN hopping $J_2 \neq 0$.

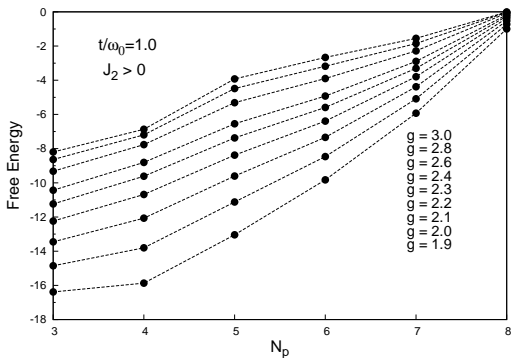


FIG. 13: Free energy versus filling with $t/\omega_0 = 1.0$ and b-p coupling g at different values. Here too $J_2 > 0$.

while n_s actually goes to zero, n_b remains finite [as follows from Eq. (23)] at a value $1/N = 1/16$ which is an artifact of the finiteness of the system. The lower critical value of g at higher values of the adiabaticity parameter t/ω_0 has already been explained in Sec. IV. Thus at half-filling, in the absence of NNN hopping, a system of hard core bosons coupled with optical phonons under-

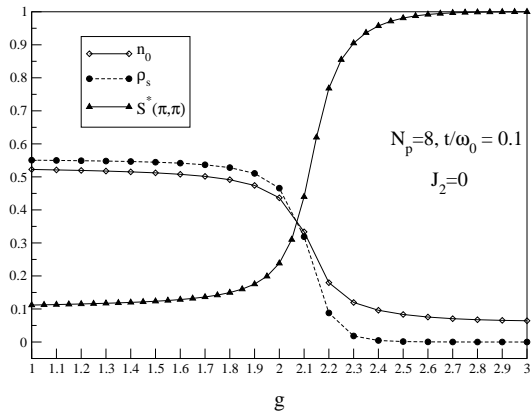


FIG. 14: Comparison of normalized structure factor $S^*(\pi, \pi)$, condensate fraction n_b , and superfluid fraction n_s for 8 particles when $J_2 = 0$ and $t/\omega_0 = 0.1$.

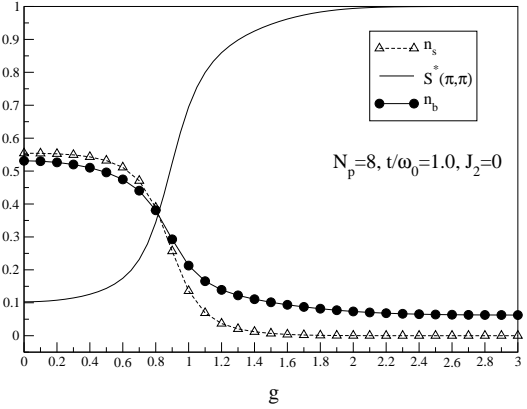


FIG. 15: Comparison of $S^*(\pi, \pi)$, n_b , and n_s for 8 particles when $J_2 = 0$ and $t/\omega_0 = 1.0$.

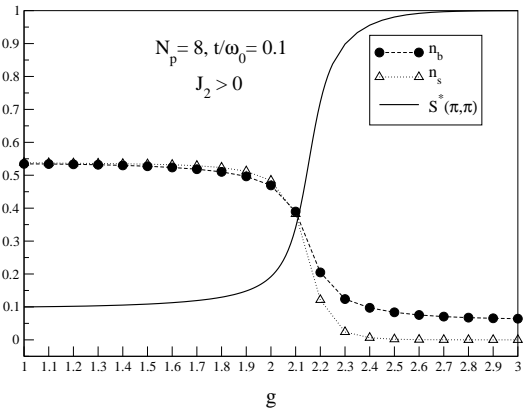


FIG. 16: Comparative plots of $S^*(\pi, \pi)$, n_b , and n_s for 8 particles when $t/\omega_0 = 0.1$, but $J_2 > 0$.

goes a transition from a superfluid state to an insulating CDW state. For a half-filled system, the presence of NNN hopping does not produce a qualitative difference in the plots, except for changing the critical value g_c of transition and that too only for adiabaticity values t/ω_0 of the order of unity. This can be seen from Figs. 16 and 17. Here also n_b and n_s behavior complements that of $S(\pi, \pi)$; the values of n_b and n_s drop noticeably when $S(\pi, \pi)$ increases sharply. These results for half-filling, with $J_2 = 0$ and $J_2 \neq 0$, were already qualitatively predicted in the mean-field analysis of Sec. III.

Away from half-filling, the system shows markedly different behavior compared to the half-filled situation. From Figs. 18 and 19, for $J_2 = 0$, although $S(\pi, \pi)$ displays a CDW transition at a critical value g_c , n_b does not go to zero, again due to finite size effects, even at large values of g . For $N_p = 5$ and $t/\omega_0 = 0.1$ ($t/\omega_0 = 1.0$), we obtain the critical value $g_c = 2.45$ ($g_c = 1.75$). From Figs. 10 and 11, we see clearly that at these critical values of g , the free energy curves become concave for $N_p = 5$. This suggests that the system is in a phase-separated state, i.e., it is an inhomogeneous mixture of CDW-state and superfluid-state. Thus away from half

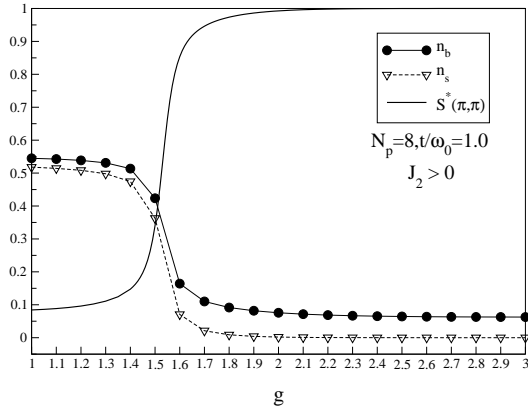


FIG. 17: Comparative depiction of $S^*(\pi, \pi)$, n_b , and n_s for 8 particles when $t/\omega_0 = 1.0$ and $J_2 > 0$.

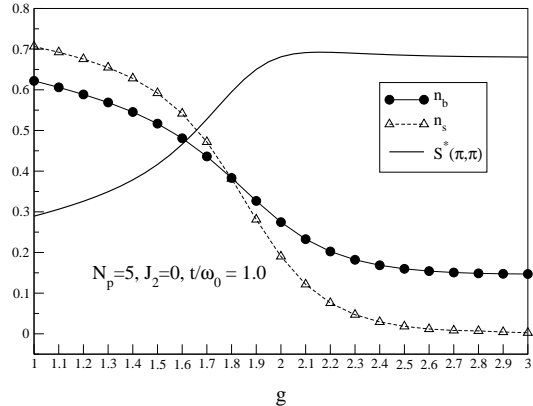


FIG. 19: Simultaneous phase transitions shown by $S^*(\pi, \pi)$, n_b , and n_s for 5 particles when $J_2 = 0$ and $t/\omega_0 = 1.0$.

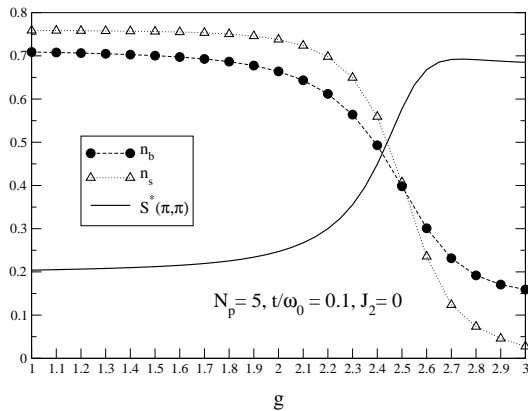


FIG. 18: Concomitant transitions depicted by $S^*(\pi, \pi)$, n_b , and n_s for 5 particles when $J_2 = 0$ and $t/\omega_0 = 0.1$.

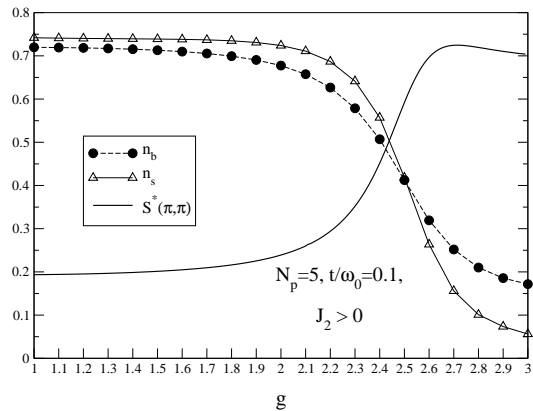


FIG. 20: Comparative study of $S^*(\pi, \pi)$, n_b , and n_s for 5 particles when $J_2 \neq 0$ and $t/\omega_0 = 0.1$.

filling, when $J_2 = 0$, our hcb-system undergoes a transition from a superfluid-state to a phase-separated-state at a critical boson-phonon coupling strength.

In the presence of NNN hopping and in the extreme anti-adiabatic limit also, the system's behavior for $N_p = 5$ is very similar to that of $J_2 = 0$ at the same adiabaticity as can be seen by comparing Fig. 20 with Fig. 18 and Fig. 12 with Fig. 10. However for t/ω_0 not too small, when NNN hopping is present, the system shows a strikingly new behavior for a certain region of the g -parameter space. Let us consider the system at $N_p = 5$, $t/\omega_0 = 1.0$, and $J_2 \neq 0$. Fig. 21 shows that, above $g \approx 1.85$, the system enters a CDW state (as can be seen from the structure factor); however, it continues to have a superfluid character as reflected by the finite value of n_s . Furthermore, Fig. 13 reveals that the system is phase-separated only above $g = 2.0$. This simultaneous presence of DLRO and ODLRO, without any inhomogeneity (for $1.85 < g < 2.1$), implies that the system is a *supersolid*. Similarly, for 6 and 7 particles as well, we find that the system undergoes transition from a superfluid to a supersolid-state and then to a phase-separated-state. This is displayed in the phase diagram given in Fig. 22.

Another point to be noted here is that, in Figs. 17 and 21 (i.e., for $t/\omega_0 = 1.0$, $J_2 > 0$, and small values of g), n_s becomes smaller than n_b . We feel that this is an artifact of the approximation used for the mass in Eq. (26).

Finally, we shall present the interesting case of $J_1 = 0$ as a means of understanding the supersolid phase in the phase diagram of Fig. 22. The physical scenario, when J_1 can be negligibly small compared to J_2 (see Ref. [24] for a one-dimensional example), and the detailed results will be published later³⁰. Here we only present the results that are relevant to the conclusions made in the above discussions. It is quite natural that, when $J_1 = 0$, all the particles will occupy a single sub-lattice for large values of nearest-neighbor repulsion. For a half-filled system, above a critical point, all the particles get localized, resulting in an insulating state. This can be seen from Fig. 23. One can see that (at $J_z/J_2 \approx 7.2$) the structure factor dramatically jumps to its maximum value, while n_s drops to zero and n_b takes the limiting value of $1/16$ for reasons discussed earlier. This shows that above $J_z/J_2 = 7.2$, the system is in a insulating state with one sub-lattice being completely full. However, away from half-filling, the system conducts perfectly while occupy-

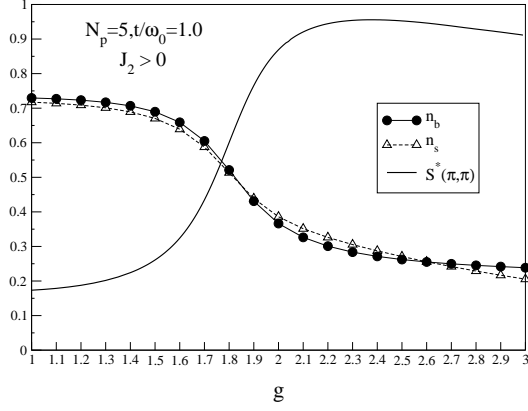


FIG. 21: Comparison of $S^*(\pi, \pi)$, n_b , and n_s for 5 particles when $J_2 \neq 0$ and $t/\omega_0 = 1.0$.

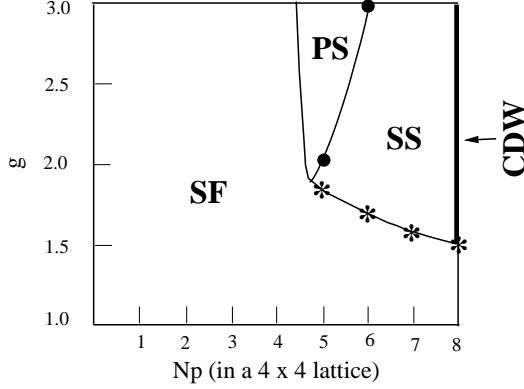


FIG. 22: Phase diagram depicting various phases for $J_2 > 0$ and $t/\omega_0 = 1.0$

ing a single sub-lattice because of the presence of holes in the sub-lattice. For instance, from Fig. 24 drawn for $N_p = 5$, we see that the structure factor jumps to its maximum value at $J_z/J_2 \approx 7.5$, while n_s drops to a finite value which remains constant above $J_z/J_2 = 7.5$. From Fig. 25 we see, based on the curvature of the free energy

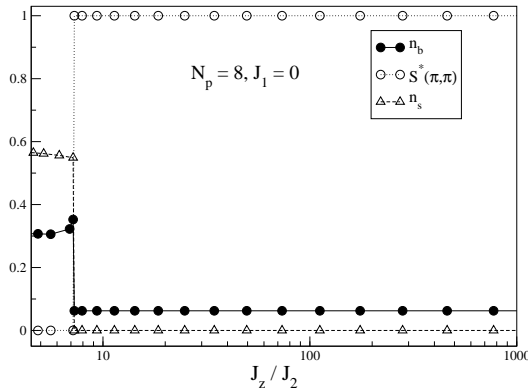


FIG. 23: Comparison of $S^*(\pi, \pi)$, n_b , and n_s for 8 particles when $t/\omega_0 = 1.0$, but $J_1 = 0$.

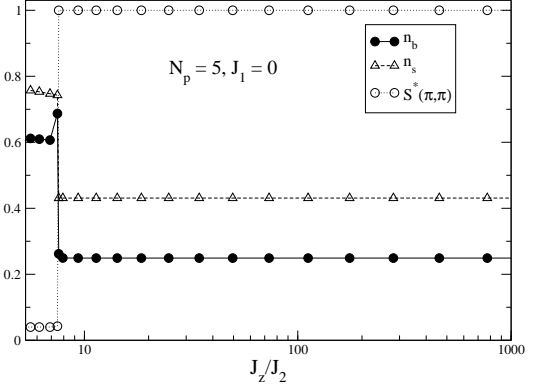


FIG. 24: Comparison of $S^*(\pi, \pi)$, n_b , and n_s for 5 particles when $t/\omega_0 = 1.0$. Here too $J_1 = 0$.

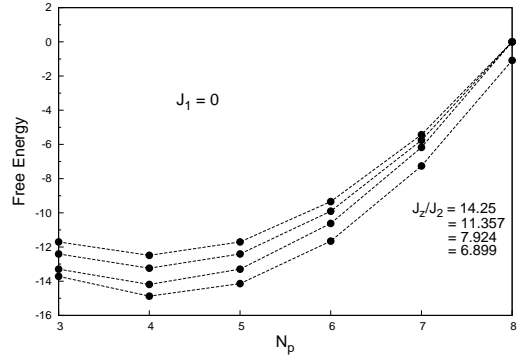


FIG. 25: Plot of free energy for different number of particles at various values of g when $J_1 = 0$.

curves, that the 5-particle system does not phase separate both above and below the transition. In fact, this single-phase-stability is true for any filling. This means that, at non-half filling and above a critical J_z/J_2 , the system is homogeneous with simultaneous existence of both DLRO and ODLRO, i.e., the system exhibits supersolidity! Thus, except for the pathological case of one particle, the system undergoes a first-order phase transition from a superfluid to a supersolid state away from half-filling.

VIII. ACKNOWLEDGMENTS

S. Datta would like to thank Arnab Das for very useful discussions regarding numerical implementation of exact diagonalization. S. Yarlagadda thanks K. Sengupta and S. Sinha for valuable discussions.

-
- ¹ M. Greiner, I. Bloch, O. Mandel, T. W. Hansch, and T. Esslinger, *Phys. Rev. Lett.* **87**, 160405 (2001).
 - ² M. Greiner, O. Mandel, T. Esslinger, T. W. Hansch, and I. Bloch, *Nature* **415**, 39 (2002).
 - ³ M. P. A. Fisher, P. B. Weichman, G. Grinstein, and D. S. Fisher, *Phys. Rev. B* **40**, 546 (1989).
 - ⁴ A. F. Andreev and I. M. Lifshitz, *Sov. Phys. JETP* **29**, 1107 (1960).
 - ⁵ G. V. Chester, *Phys. Rev. A* **2**, 256 (1970).
 - ⁶ A. J. Leggett, *Phys. Rev. Lett.* **25**, 1543 (1970).
 - ⁷ O. Penrose, *Philos. Mag.* **42**, 1373 (1951).
 - ⁸ O. Penrose and L. Onsager, *Phys. Rev.* **104**, 576 (1956).
 - ⁹ E. Kim and M. H. W. Chan, *Nature (London)* **427**, 225 (2004).
 - ¹⁰ E. Kim and M. H. W. Chan, *Science* **305**, 1941 (2004).
 - ¹¹ D. Heidarian and K. Damle, *Phys. Rev. Lett.* **95**, 127206 (2005).
 - ¹² R. G. Melko, A. Paramekanti, A. A. Burkov, A. Vishwanath, D. N. Sheng, and L. Balents, *Phys. Rev. Lett.* **95**, 127207 (2005).
 - ¹³ S. Wessel and M. Troyer, *Phys. Rev. Lett.* **95**, 127205 (2005).
 - ¹⁴ P. Sengupta, L. P. Pryadko, F. Alet, M. Troyer, and G. Schmid, *Phys. Rev. Lett.* **94**, 207202 (2005).
 - ¹⁵ G. Pupillo, A. Griessner, A. Micheli, M. Ortner, D.-W. Wang, and P. Zoller, *Phys. Rev. Lett.* **100**, 050402 (2008).
 - ¹⁶ C. M. Varma, *Phys. Rev. Lett.* **61**, 2713 (1988).
 - ¹⁷ A. Taraphder, H. R. Krishnamurthy, Rahul Pandit, and T. V. Ramakrishnan, *Phys. Rev. B* **52**, 1368 (1995).
 - ¹⁸ R. Ramakumar and S. Yarlagadda, *Phys. Rev. B* **67**, 214502 (2003).
 - ¹⁹ E. R. Gagliano, E. Dagotto, A. Moreo, and F. C. Alcaraz, *Phys. Rev. B* **34**, 1677 (1986); **35**, 5297 (1987).
 - ²⁰ S. Datta, A. Das, and S. Yarlagadda, *Phys. Rev. B* **71**, 235118 (2005).
 - ²¹ T. Holstein, *Ann. Phys. (N.Y.)* **8**, 343 (1959).
 - ²² I.G. Lang and Yu.A. Firsov, *Zh. Eksp. Teor. Fiz.* **43**, 1843 (1962) [*Sov. Phys. JETP* **16**, 1301 (1962)].
 - ²³ J. E. Hirsch and E. Fradkin, *Phys. Rev. B* **27**, 4302 (1983).
 - ²⁴ S. Yarlagadda, arXiv:0712.0366v2.
 - ²⁵ S. Robaszkiewicz, R. Micnas, and K. A. Chao, *Phys. Rev. B* **23**, 1447 (1981).
 - ²⁶ G. D. Mahan, *Many-Particle Physics*, (Plenum Press, New York, 1981).
 - ²⁷ K. Huang, *Statistical Mechanics*, (John Wiley & Sons, Inc., New York, 1987) 2nd ed.
 - ²⁸ Robert Roth and Keith Burnett, *Phys. Rev. A* **68**, 023604 (2003)
 - ²⁹ P.M. Chakin and T.C. Lubensky, *Principles of Condensed Matter Physics*, (Cambridge University Press, Cambridge, United Kingdom, 1998).
 - ³⁰ S. Datta, S. Yarlagadda, and P. B. Littlewood (to be published).